

Ground State and Transition State Contributions to the Rates of Intramolecular and Enzymatic Reactions

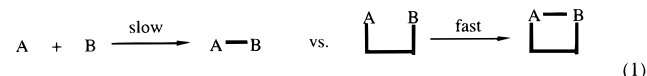
THOMAS C. BRUCE* AND
FELICE C. LIGHTSTONE¹

Department of Chemistry and Biochemistry, University of California, Santa Barbara, California 93106

Received May 4, 1998

Introduction

Reactions within enzyme–substrate (E·S) complexes share with intramolecular reactions the close proximity of reactants. This proximity effect results in a much larger numerical value of the rate constants when compared to the rate constants of the corresponding bimolecular reaction (eq 1). In essentially strain-free intramolecular

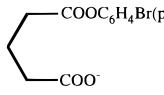
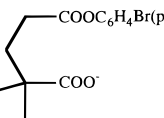
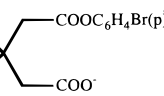
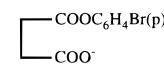
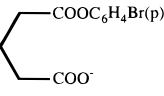
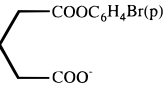
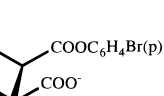


reactions, rate enhancements of 10^8 M have been observed (Table 1).² Intramolecular reactions where severe ground state strain is relieved upon formation of the transition state are known to be as large as 10^{16} M.³ Kirby⁴ has compiled a compendium of intramolecular reactions and has pointed out the relationship of rate to exothermicity. The importance of ground state conformations and the lack of translational entropy in intramolecular and enzymatic reactions have drawn attention from Menger⁵ and ourselves, while Jencks and Page⁶ have offered an explanation based on entropic driving forces stemming from the freezing out of motions and the dampening of vibrational frequencies in the transition state. Houk,⁷ in

Thomas C. Bruce attended the University of Southern California (B.S., 1950; Ph.D., 1954) and received his postdoctoral training at UCLA after dropping out of high school in the eleventh grade (1943) and serving in the military. Prior to joining the faculty of the University of California at Santa Barbara in 1964, Professor Bruce held faculty positions at Yale, John Hopkins, and Cornell Universities. An inventor of the term bioorganic chemistry, he has contributed importantly to many areas of mechanistic chemistry dealing with problems important in biochemistry. His accomplishments have been recognized by a number of prestigious awards.

Felice C. Lightstone was born and raised in Chicago, IL. She received B.S. degrees in electrical engineering and honors biology from the University of Illinois. After completing her M.S. degree in electrical engineering from the University of Illinois, she chose to pursue a Ph.D. in computational chemistry at the University of California at Santa Barbara. She completed her graduate work in March 1998 and is presently a Postdoctoral Research Scientist at Lawrence Livermore National Laboratories in Livermore, CA. Her interests are in studying biochemical reaction mechanisms using computational methods, including the mechanisms of DNA repair enzymes.

Table 1. List of Monophenyl Esters Used and Their Relative Rate Constants

	k_{rel}
$\text{CH}_3\text{COO}^- + \text{CH}_3\text{COOC}_6\text{H}_4\text{Br(p)}$	1.0
I 	$\sim 1 \times 10^3$ M
II 	$\sim 3.6 \times 10^3$ M
III 	$\sim 1.8 \times 10^5$ M
IV 	$\sim 2.3 \times 10^5$ M
V 	$\sim 2.7 \times 10^5$ M
VI 	$\sim 1.3 \times 10^6$ M
VII 	$\sim 8 \times 10^7$ M

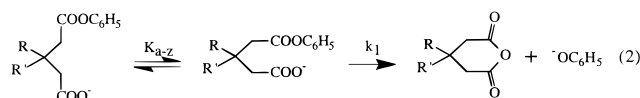
a scholarly study, has provided a correlation between rate constants for certain lactonization reactions and transition state stabilization. We provide here an account of our recent computational results^{8–10} dealing with the driving forces for enzymatic and intramolecular reactions.

We introduce⁸ the term near attack conformation (NAC) to define the required conformation for juxtaposed reactants to enter a transition state (TS). The greater the mole fraction of reactant conformations that are present as NACs, the greater the rate constant. Rate constants for bond making and breaking in enzymatic reactions depend on, (i) the fraction of E·S present as NACs, (ii) the change in solvation of reactant species within the NAC, as compared to water, and (iii) electrostatic forces¹¹ which can stabilize the TS. The latter may include hydrogen bonds and metal ligation. Covalency in metal ligation and hydrogen bonding (low barrier hydrogen bonding¹²) most probably are introduced in the ground state. These features are best appreciated when ground state conformations and TS structures can be examined separately.

Near Strain Free Intramolecular Reactions

Ground State Conformations. The relationship of the relative stability of NACs and rate constants have been studied⁸ with a series of intramolecular reactions of dicarboxylic acid monoesters which yield five- and six-

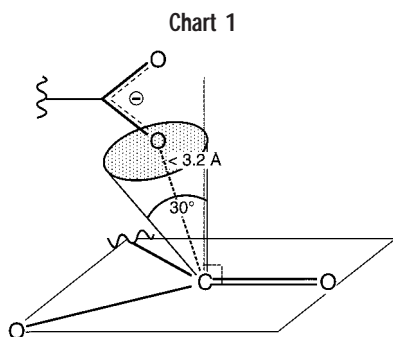
membered cyclic anhydrides (eq 2 and Table 1).² The



non-NACs

NACs

procedure we have employed should be of general use when one wishes to know the mole fraction of some given conformation from all conformations in a system. The first step is to define the geometry of this given conformation. For cyclic anhydride formations with the monoesters of Table 1, the geometry of the NAC was determined to be as shown in Chart 1.⁸ The NAC is a genuine ground



state conformation with reaction centers properly aligned for reaction but at $\sim 3 \text{ \AA}$ separation, where bond making and breaking have not been initiated, and the carbonyl carbon remains sp^2 . Once the NAC has been defined, the problem can be viewed as consisting of two parts: (a) identifying ground state conformational equilibria, including formation of NACs, and (b) locating the transition state in the conversion of the NAC to product.

Conformations of each monoester of Table 1 were identified by first creating 10 000 to 40 000 spatial isomers by using Saunders' stochastic search method^{13,14} through MM3(92)¹⁵ and discarding duplicates and those structures containing imaginary vibrational frequencies. The remaining unique structures were then individually energy minimized and represent a set of stable conformations. In this manner, we obtained for each monoester a collection of the various conformations, conformational energies, and conformational thermodynamic parameters (G° , H° , and S°). The conformational energies account for such structural aspects as bond eclipsing and gauching, angle distortions, etc. Conformations possessing the features of a NAC (Chart 1) were then identified. Using the energies of the conformations and a weighted Boltzmann distribution, we calculated the mole fraction (P) of conformations present as NACs for each ester. Figure 1 provides the energy distribution of the conformers of the various esters of Table 1. Figure 2 is a plot of \log of P vs the \log of the experimental relative rate constants (k_{rel}) for anhydride formation. One can conclude from the slope (0.94) of Figure 2 that there is a direct linear free-energy relationship between the \log of the fraction of conformations present as NACs and ΔG^\ddagger . Thus, *the rate constants for the reactions of the esters of Table 1 are*

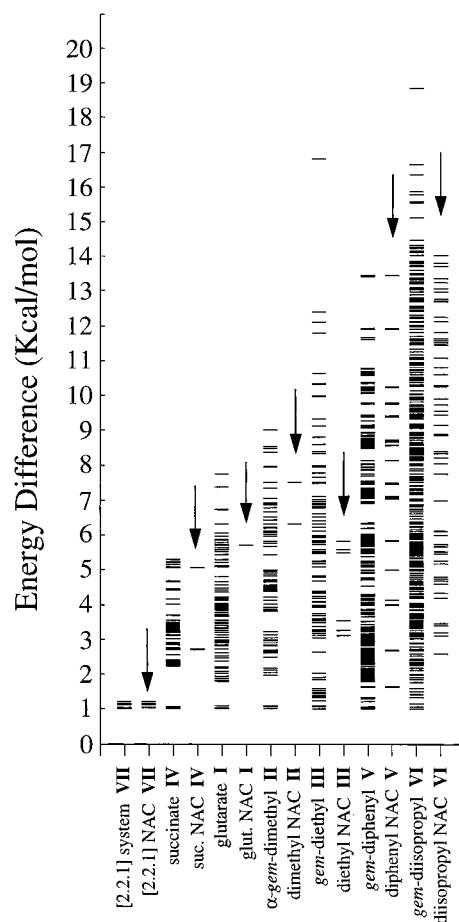


FIGURE 1. Plots of differences in MM3 final energies of all local minimum conformations relative to the lowest energy ground state conformation for each ester in Table 1.⁸ Those esters to the right of glutarate are β -geminally substituted glutarate esters, unless marked. Those esters to the left of glutarate are the rotationally more constrained esters.

directly dependent upon the mole fraction of the ground state of each ester present as NACs. When the ground state consists of only NACs, the rate enhancement is 10^8 M. Figure 3 shows that the values of P for these esters are related to the change in ΔH^\ddagger for NAC formation rather than the change in phase space entropy ($T\Delta S^\ddagger$). Thus, the activation free energy (ΔG^\ddagger) is a function of the ground state standard enthalpy (ΔH^\ddagger) for NAC formation. Illuminati and Mandolini,¹⁶ in their classical studies of intramolecular lactonizations, offered support for entropy of activation (ΔS^\ddagger) as the important factor in the free energy of activation (ΔG^\ddagger). Reinterpretation¹⁷ of these experimental data establishes that ring closure in intramolecular lactone formation with formation of five- and six-membered rings is driven by a favorable ΔH^\ddagger .

In the cartoon of Chart 2, the black and gray balls represent the reactants of a bimolecular reaction. Covalently connecting the black and gray balls by a three atom bridge provides an intramolecular reactant. In going from the intermolecular reaction to the intramolecular reaction, there is a loss of translational motion. Bruice and Benkovic provided experimental data which showed that for a series of 40 reactions, the division of the

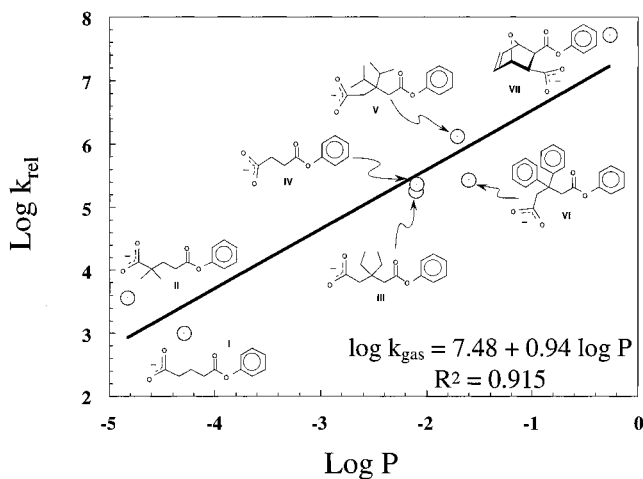


FIGURE 2. Log of the relative rate constants (k_{rel}) for anhydride formation from mono-*p*-bromophenyl esters vs the log of the probability (P) for NAC formation of each monopheyl ester in Table 1.⁸

experimental entropy of activation ($T\Delta S^\ddagger$) by the kinetic order provides, on average, 4.6 kcal/mol.¹⁸ This is equivalent to a $\sim 2 \times 10^3$ rate enhancement due to the change in translational entropy upon conversion of a bimolecular reaction to an intramolecular reaction. Rotation around the bonds connecting the black and gray reactants in the intramolecular model allows the existence of many conformers. Each conformer is a separate entity existing at a local energy minimum and characterized by its bond angles and internal energy. The same restrictions in translational and rotational motion are shared by the various conformers. The intramolecular reaction to provide the cyclic product can take place only from near attack conformers (NAC). If the NACs are not inherently stable, work is required to bring the reacting centers together before TS can be entered. This is an expenditure of enthalpy.

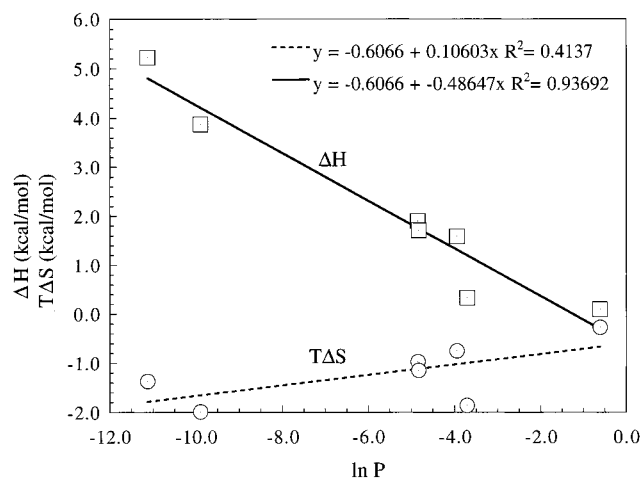
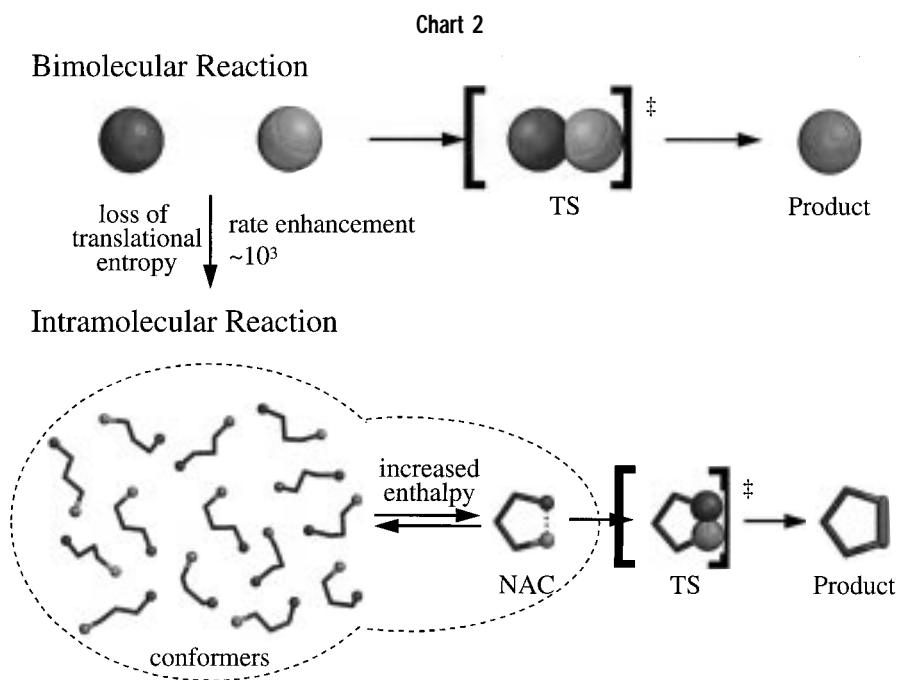


FIGURE 3. Phase space calculated thermodynamic entropy change ($T\Delta S^\ddagger$) and internal energy change (in this case, ΔE can be assumed to be ΔH^\ddagger) to attain a near attack conformation (NAC) vs the natural log of the probability of being in a NAC.⁸

Transition State (TS) Structures. In anhydride formation from the esters of Table 1, the ground and transition states are anionic. There are sometimes only minor differences between the structures of anionic ground states when calculated by semiempirical quantum mechanical (QM) methods and by *ab initio* QM methods with or without diffuse functions. However, this is not true in the calculation of anionic TS structures where the correct basis set with diffuse functions must be used to determine correct geometries and energies.^{19,20} We employed⁹ the energy gradient method at the RHF/6-31+G(d) level of theory (Gaussian programs²¹) on monoglutarate (**I**), -succinate (**IV**), and -3,6-endo- Δ^4 -tetrahydrophthalate (**VII**) esters. Because *ab initio* calculations are very costly in time, only these three representative esters were studied. We find the TS structures, in anhydride formation from **I**,



IV, and VII, to be essentially identical; they possess essentially the same bond distances and angles (Figure 4).

In the arguments of entropy as being the driving force for enzyme catalysis and intramolecular reactions, it has been proposed that the restriction or dampening of low-frequency vibrations allows the attainment of a more favorable entropy of activation.^{6,22} However, little has been done to calculate and verify these speculations. One might feel comfortable believing that when two molecules, each having three degrees of translational motion and three degrees of rotational motion, meet and form an ES complex, the complex will have converted the six extra degrees of motion to new vibrations at the interface of the two molecules, increasing the total number of vibrations. Why then would moving from the complex to the transition state dampen or restrict these existing vibrations? This concept seems to be widely accepted. Using *ab initio* intrinsic reaction coordinate (IRC) calculations in the gas phase, the intramolecular reaction of an anion ($-\text{CO}_2^-$) with a neutral substrate ($-\text{CO}_2-\text{Ph}$) provides an intramolecular ion-molecule complex (IIMC) for reactions of I and IV and a tetrahedral intermediate (TI) for reaction of VII (eq 3).

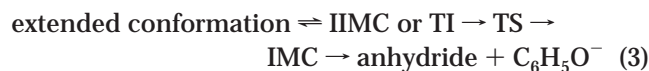


Figure 5 is a graphical representation of the calculated vibrational frequencies for the TSs and the IIMCs (or TI). The imaginary (negative) frequencies characterize the transition states. We find that the total number of frequencies does not change in going from the IIMC (or TI) to the TS for each ester. Knowing that the lower frequencies contribute more to the entropy of the structures and following the Page and Jencks criteria of frequencies lower than 1000 cm^{-1} having a significant effect on the entropy of activation,⁶ the number of lower frequencies remains constant in going from the IIMC (or TI) to the TS. The other implication from the Page and Jencks speculations⁶ is that the larger the experimental rates, the more frequencies will have to be dampened out. Since we cannot compare the absolute number of frequencies between compounds, we have taken the ratio between the number of low frequencies (below 1000 cm^{-1}) and the total number of frequencies. The ratios of the IIMCs (TI) or the TS low frequencies to the total number of frequencies for the anhydride formation of I, IV, and VII are 0.49, 0.51, and 0.55, respectively. The trend of these ratios is that the faster the reaction, the more low-frequency vibrations. So, whether the frequencies are compared within a monophenyl ester or the ratio of low frequencies to total frequencies is compared between esters, we do not observe any dampening or restriction or freezing out of the low-frequency vibrations. Therefore, by the criteria of superimposable TSs and the lack of evidence for frequency changes in the TSs in the direction of increasing rate, we conclude that the structures of the TSs do not contribute to the different rate constants of Table 1.

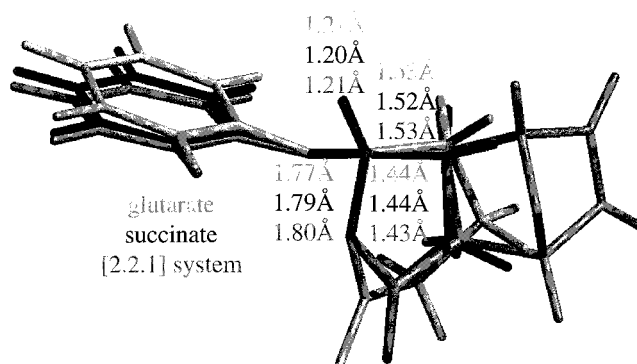


FIGURE 4. An overlay of the transition states of anhydride formation from monophenyl esters of glutaric, succinic, and 3,6-endoxo- Δ^4 -tetrahydrophthalic acid. The black figure is the transition state of succinate, the middle gray figure is the transition state of 3,6-endoxo- Δ^4 -tetrahydrophthalate, and the light gray figure is the transition state of glutarate. Where the ester moiety overlaps, the structure is shown in black as the succinate. The shown bond lengths are shade coded with the figure.⁹

Any differences in activation energies for $\text{NAC} \rightarrow \text{TS}$ must reside in small differences in the NAC structures for the three esters—a feature of the ground state. Such a difference is found in the distances between carboxylate oxygen and ester carbonyl carbon for the NACs of the three esters (3.20 \AA for I, 3.08 \AA for IV, and 2.93 \AA for VII). Some finite difference in activation energies for $\text{NAC} \rightarrow \text{TS}$ for the three esters is to be expected. The contribution of this feature to the overall ΔG^\ddagger would be in the same order as the overall order of ΔG^\ddagger , $\text{I} > \text{IV} > \text{VII}$, respectively.

The energy difference between NAC and TS cannot be directly calculated. The closest structure to a NAC obtained by *ab initio* gas phase optimization is an intramolecular carboxylate ion-molecule complex (IIMC) whose formation is dictated by the need to stabilize a

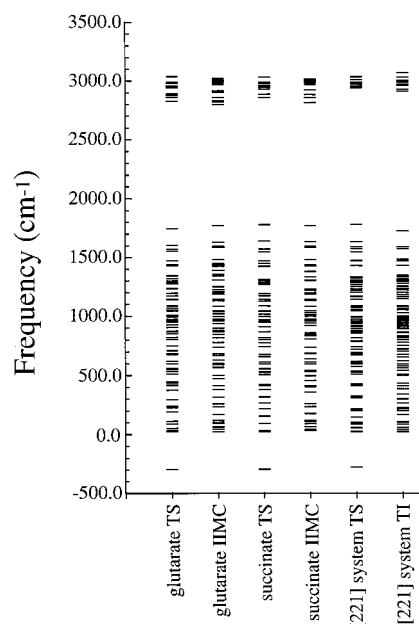


FIGURE 5. Frequencies for both the intramolecular ion-molecule complex (IIMC) and transition state (TS) for the glutarate, succinate, and 3,6-endoxo- Δ^4 -tetrahydrophthalate monophenyl ester reactions. As observed, the transition states have one imaginary frequency.⁹

carboxylate anion in the gas phase. Thus, one can only determine the energy difference between the IIMC and the TS. The IIMC is further along the reaction path than is the NAC. Comparison of activation parameters for the conversion of IIMC \rightarrow TS in the reactions of esters **I** and **IV** shows very little change in $T\Delta S^\ddagger$ compared to the change in ΔH^\ddagger . Thus, formation of ground state NACs and TS is under enthalpic control.

The rate constants for the reactions of Table 1 were determined in solution such that one would like to compute activation energies in solution. IIMCs most likely do not exist as energy minima in solution but rather as metastable species along the reaction coordinate from NAC to TS (eq 4). A cartoon of the reaction coordinates



for the processes of eq 4 in solution is provided in Figure 6. Superimposed on this cartoon is one which depicts moving the process from solution to the gas phase. In the cartoon, the gas phase and solution TSs are superimposed, representing like stabilities and structures. The assumption is made that desolvation provides the same increase in energies of all single negatively-charged species. The energy differences between IIMC and TS are seen to decrease in the order **I** < **IV** < **VII**, reflecting the relative ground state energies.

Unfortunately, reliable solvation calculation methods are still in their challenging stages of development such that the ability to quantitate the conclusions shown in Figure 6 is questionable. A common approach to the calculation of reaction energies in solution is to first determine the gas phase *ab initio* TS and nearest local minima structures on reactant and product sides of the TS (in our case IIMC and IMC), assume the structures do not change in going to the solution phase, and then calculate the energies of these structures in solution. We used the Hartree-Fock method {HF/6-31+G(d) level of theory, including diffusion functions}²¹ in conjunction with the intrinsic reaction coordinate (IRC)^{23,24} method

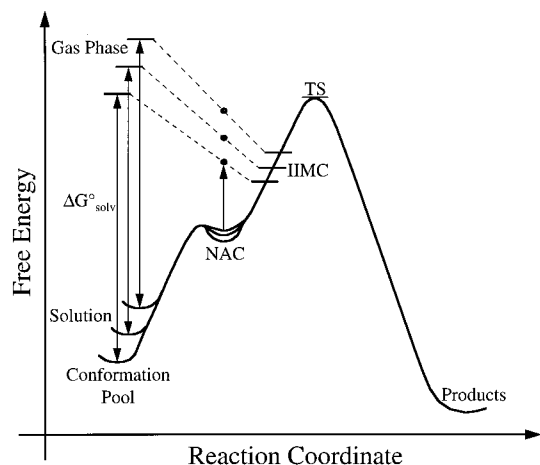


FIGURE 6. A cartoon of the proposed solution reaction coordinate. Overlaid is the gas phase reaction coordinate with the transition state as a reference point.

to determine the structures of TS, IIMC, and IMC in the gas phase. The single point energies in solution are calculated by the continuum solvent method (SCIPCM),²⁵⁻²⁷ Results of such calculations are useful for providing general trends, but may not be good enough to allow rigorous discussion of the results. In our energy calculations in solution, we also used a hybrid density functional theory method (DFT, B3LYP)²⁸ in conjunction with a solvent continuum method (B3LYP/6-31+G(d), B3LYP/6-31+G(d)/SCRF-SCIPCM). Upon transferring from gas phase (HF/6-31+G(d)) to solution (HF/6-31+G(d)/SCRF-SCIPCM), energy differences between IIMC and TS increase substantially (32%, 48%, and 57%, respectively). These differences decrease by a factor of ~ 2 using just the DFT single point energy calculations. But, when the continuum solvent method is combined with the DFT method, the energy differences increase compared to DFT, however, are lower than HF gas phase energies. Thus, the exact activation barriers are different with different methods of calculation. The overall trend, however, has the activation barriers in solution decreasing going from IIMC of **I** \rightarrow TS, IIMC of **IV** \rightarrow TS, to TI of **VII** \rightarrow TS. Since TI is further along the reaction coordinate than is IIMC, the activation barrier from TI \rightarrow TS is expected to be smaller than that for IIMCs \rightarrow TS.

We are only left with comparing the energy differences between IIMC and TS for esters **I** and **IV**. As anticipated in the cartoon of Figure 6, this energy difference is greater for ester **I** than for ester **IV**. Even this single comparison, however, is in doubt. The single point continuum solvent calculations assume that the states immediately preceding and following the transition state and the TS structure itself do not change upon going from the gas phase to solution. For a charged system, such as these monoester reactions, the gas phase geometry is certainly not the same as the solution geometry.²⁹ More importantly, the gas phase minima of IIMC and IMC may not even exist in solution. The answer to this problem is then to optimize IIMCs and TSs in a continuum solvent method. Diffuse functions are necessary for these negatively charged monophenyl esters and TSs. The continuum solvent method systems are very costly (in time) when diffuse functions are used, and due to difficulty in converging, such calculations are often not successful.

What General Principles, Learned in the Study of the Model System of Table 1, Can Be Applied to Enzyme Catalysis? The data of Table 1 are offered, in many general biochemistry and advanced texts, to show the importance of the increase in entropy on bringing together reactants and stabilization of the transition state. This interpretation has had a profound influence on how enzymologists view enzyme catalysis. Thus, it is often stated in the biochemical literature that the entropy factor in bringing together of substrate and catalyst at the active site may be expected to result in a rate enhancement of 10^8 . We have now shown that the driving force for the rate enhancements of Table 1 is enthalpic (in the ground state and activation, ΔH^\ddagger and ΔH^\ddagger).

A **rational stance for the enzymologist** is to consider driving forces for enzymatic reactions to arise from both ground state and transition state features. In the formation of the collective E·S species, entropy increases because translational motion is lost. Formation of NACs involves combined motions of both S and E. In our model system, formation of NACs is under enthalpy control. The frequency of formation of NACs in the enzymatic reaction is under control of the preorganization of the active site of the enzyme. It is probably not possible to judge *a priori* the relative importance of enthalpy and entropy to NAC formation in the ES complex. Using the data of Table 1 as a guide, ground state features can provide (dependent on the complexity of the reaction) rate enhancements of $\sim 10^8$ in strain free enzymatic reactions (greater if there is orbital overlap⁵). One would suppose that the free energy of reaction going from NAC \rightarrow TS can then be dominated by either entropy or enthalpy, depending upon the nature of the reaction. Electrostatic forces and the heterogeneous milieu of the active site may provide up to another 10^8 -fold rate enhancement due to stabilization of the TS. The most efficient enzymatic reactions should have a large equilibrium constant for ES formation, a mole fraction of ES present as NACs approaching unity, and the free energy of the TS significantly lowered by electrostatic interactions, which are accentuated by the heterogeneous milieu of the active site.

Ground State and Transition State Structures in Enzymatic Reactions

Computational observation of the periodicity of NAC formation in the E·S complex is now possible. The starting point for all such calculations is an experimentally determined structure (X-ray or NMR) of E·S complex at high resolution {or a like structure of E·I from which E·S can be generated}. Energy minimization followed by analysis of data from extensive molecular dynamics (MD) simulations allows the identification of NAC structures.

Calculation of E·TS structures is carried out as follows. If function A of the enzyme reacts with function B of the substrate to provide TS_{AB} , then the gas phase structure of TS_{AB} is calculated by *ab initio* methods, which can also provide heavy atom isotope effects. One may safely conclude that the computed gas phase TS and enzyme bound TS share the same structure when their isotope effects are equivalent (or nearly so). If there are no experimental isotope effects for comparison, but chemical evidence indicates that the TS is not significantly altered upon transfer from the gas phase to solution, one may use the following procedures. Semiempirical QM methods (AM1, PM3) are used to generate a TS that is comparable to the *ab initio* TS. The semiempirical TS is incorporated into a cut-away portion of the enzyme representing the active site, and the TS and surrounding amino acid side chains are optimized. The optimized portion of the enzyme with a newly optimized TS is then reconnected into the enzyme to generate the E·TS structure. However determined, the E·TS structure, after

minimization, is subjected to lengthy MD simulations to provide the numerous $E^1\cdot TS$, $E^2\cdot TS$, ..., $E^n\cdot TS$ structures. Changes in interactions of components on $E\cdot S \rightarrow E\cdot TS$ can be observed such that concepts as transition state stabilization and others can be evaluated.

Computational times increase dramatically with the size of the enzyme and the complexity of the reaction process. For this reason, ideal targets for study are enzymes of low mass catalyzing very simple displacement reactions. Reactions undergoing study in this laboratory include one step S_N2 displacements on sp^3 carbons and hydride reductions of sp^2 carbonyl carbons. The S_N2 reactions under investigation involve nucleophilic attack of catechol monoanion on the methyl of *S*-adenosylmethionine (catechol *O*-methyltransferase, COMT) and attack of an $Asp-CO_2^-$ on a carbon of 1,2-dichloroethane with expulsion of Cl^- (haloalkane dehalogenase). There is no doubt that the driving force for both these S_N2 enzymatic reactions is attributed to a proximity effect inherent to the NAC, desolvation of oxyanion nucleophiles in NAC structures, and some small contributions from TS stabilization. The *ab initio* calculated isotope effects of a model match those experimentally determined for the COMT enzymes,³⁰ and thus, the QM computed TS has the same geometry as does the enzymatic reaction. Much the same is true of NAD^+ reduction by formate where the computed isotope effects for a model reaction are very close to those determined experimentally for formate reductase.²⁹

The S_N2 displacement of Cl^- from 1,2-dichloroethane (DCE) by $Asp124-CO_2^-$ at the active site of *Xanthobacter autotrophicus* haloalkane dehalogenase (Scheme 1) was chosen on the basis that (i) TS structures for S_N2 displacements of anionic leaving groups by anionic nucleophiles are comparable in gas and liquid phases³¹ and (ii) a crystallographic structure of the enzyme is available at 1.9 Å,³² and a structure of the enzyme with DCE at the active site is available at 2.4 Å.³³ Chart 3 is a stereoview of the original crystal structure of the enzyme-substrate (E·S) complex. Molecular dynamics simulations (AMBER 4.1³⁴) of the E·S and E·TS were run at constant temperature for 540 ps.¹⁰ Chart 4 represents orthogonal views of an MD snapshot of a NAC structure of the E·S complex. The substrate is shown to be in a *gauche* conformation (as predicted from the *ab initio* reaction coordinate for the reaction of $CH_3CO_2^-$ with DCE³⁵) while the crystal structure shows DCE in a *trans* conformation.³³ The NAC structure of Chart 4 is formed when Water323 dissociates from the nucleophilic oxygen (OD2) of $Asp124-CO_2^-$, and the latter approaches to 3 Å from C(1) of DCE. In this NAC structure, OD2 of $Asp124-CO_2^-$ is in-line with the departing Cl(1) which is hydrogen bonded to the indole HN of Trp125. The E·TS structure was constructed as follows. The *ab initio* and semiempirical (PM3³⁶) transition states³⁵ for the S_N2 displacement of Cl^- from DCE by $CH_3CO_2^-$ are much alike and closely resemble the TS in solvent. A model for E·TS consisted of the PM3 generated TS surrounded by the 14 amino acids that make up the active site.³⁷ This model structure was optimized and placed back into the enzyme with the overlapping

Chart 3

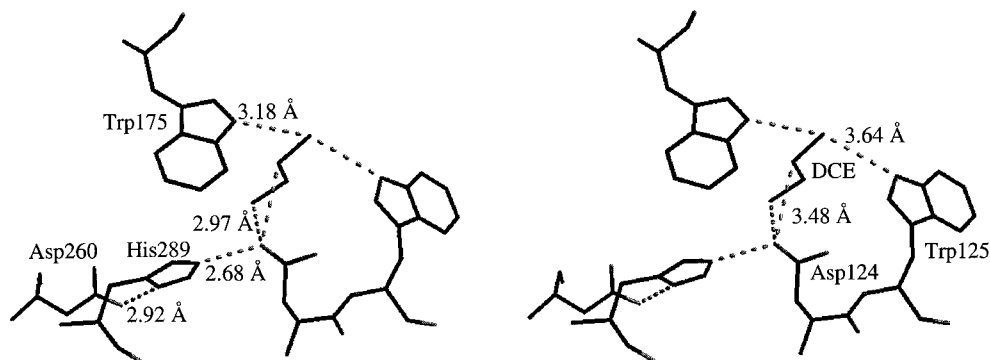


Chart 4

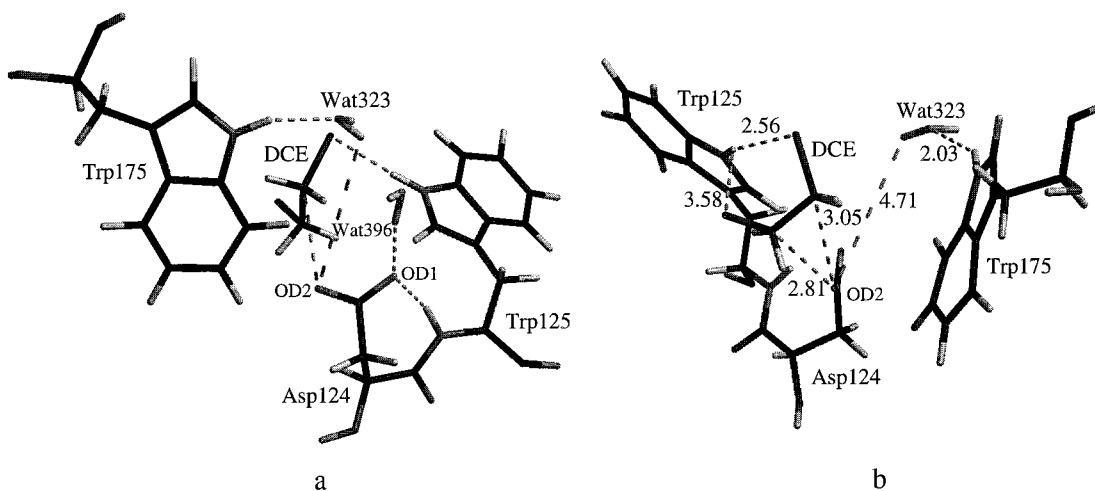
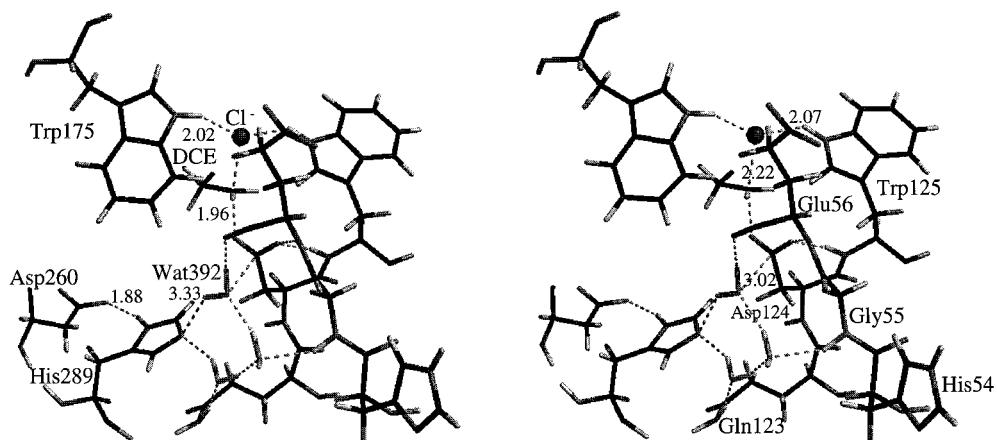


Chart 5

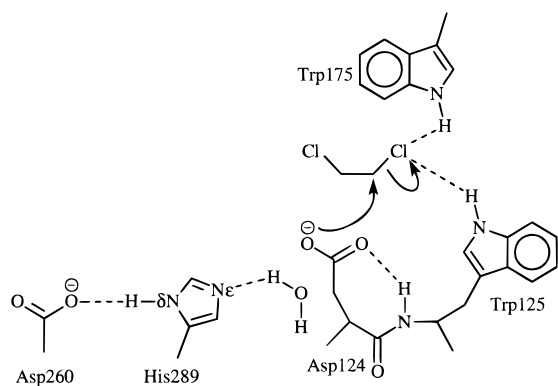


parts of the enzyme deleted to provide the complete E·TS.³⁷ Throughout the MD simulation of E·TS, the TS moiety was maintained by applying large force constants on the making and breaking bonds and associated $O^{\delta-} \cdots C \cdots Cl^{\delta-}$ angle. Chart 5 is a stereoview snapshot of the MD simulated E·TS. Trp125 which is hydrogen bonded to the chloro substituent in E·S is joined by Trp175 in hydrogen bonding to the leaving chloride in E·TS. Most interesting is the finding that, during the simulation of the TS, a hydrogen bonding matrix forms which includes three water molecules. Water323 and Water396 are held in such a manner that they exactly position a third

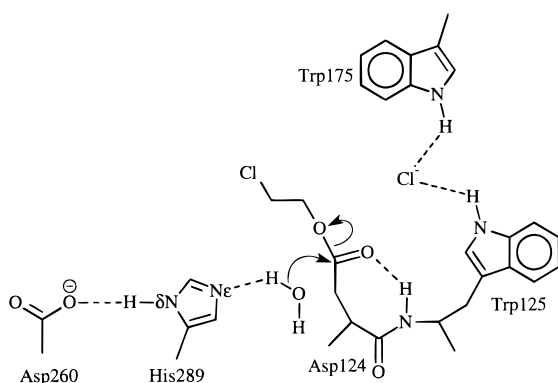
Water392 as a nucleophile to attack the ester carbonyl of Asp124-CO₂-CH₂CH₂-Cl which is formed after Cl⁻ departs from TS (Scheme 2). Thus, accompanying the formation of the TS for the first step of the reaction is the formation of the ground state triad Asp260-CO₂⁻⋯H-His289-N⋯H₂O392 (Chart 5) for hydrolysis of the intermediate ester in the second step of the reaction (Scheme 2), an example of inseparable ground and transition states.

NAC Formation by the Anisotropic Motions of Enzyme Bound NAD(P)H. 1,4-Dihydronicotinamides possess two quasi-boat conformations that are interconvertible by a wagging motion such that H_R is axial in one

Scheme 1



Scheme 2



conformation and H_S is axial in the other (Chart 6). Examination of the MD simulations of dehydrogenase enzymes with substrate and NAD(P)H at the active site shows that only one of the two possible quasi-boat conformations exists.^{38–41} In this conformation, the bending is in the direction of the substrate. Thus, in enzymatic reactions where H_R is transferred as hydride from NAD(P)H to substrate, the quasi-boat conformation has H_R axial, and in a similar manner, when H_S is transferred to substrate, H_S is axial. This anisotropic character is brought about by bulky substituents (lactate dehydrogenase, Ile249 and Val136; dihydrofolate reductase, Phe102; malate dehydrogenase, Ala245 and Leu157; glyceraldehyde-3-P dehydrogenase, Ile12 and Tyr317; horse liver alcohol dehydrogenase, Val203) which are located on the face of the dihydropyridine ring distal to the substrate and axial hydrogen (Chart 7).³⁹ The quasi-boat conformations calculated by *ab initio* methods are characterized by $\alpha_C > \alpha_N$ as seen in Figure 7.²⁹

The NAC structures are associated with formation of the quasi-boat conformation. Thus, in MD simulations with dog-fish lactate dehydrogenase³⁹ containing pyruvate and NAD(P)H at the active site, the distance between the

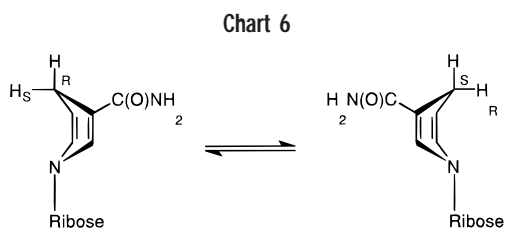


Chart 6

Chart 7

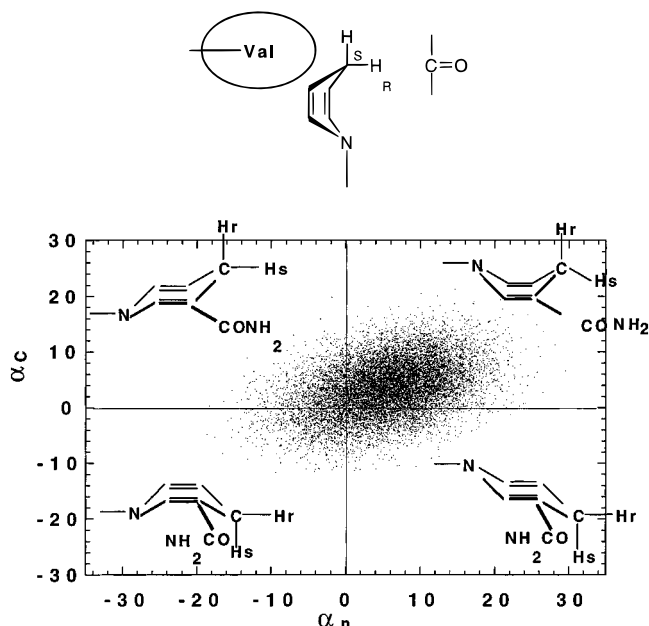


FIGURE 7. Conformational distribution of the puckering angles α_C and α_N of the NADH for subunit 1 of horse liver alcohol dehydrogenase during 1500 ps molecular dynamics run. The centers of the populations of α_C and α_N are at 4° and 6°, respectively. Forty percent of the sampling population of α_C is beyond 5°, and 8% of the sampling population of α_C is beyond 10°. The H_R hydrogen is in the axial position.⁴¹

transferring H_R and pyruvate carbonyl is 2.5 Å when the dihydropyridine ring is planar and 1.5 Å when in the boat form. In the dehydrogenases which have been examined, the bent conformation with axial- H and substrate carbon in close proximity (the NAC) are present the majority of the time (Figure 7).^{39,41} (An exception is formate reductase, work in progress.) The closeness of approach of reactants in these NAC structures, and the lessened bond energy of C(4)–axial- H as compared to C(4)–equatorial- H ,³⁹ is proposed to provide a kinetic advantage to hydride transfer.

These studies were supported by grants in aid from the National Institutes of Health, the Petroleum Research Fund of the American Chemical Society, and the National Science Foundation.

References

- (1) Current address: Biology and Biotechnology Research Program, P.O. Box 808, L-452, Lawrence Livermore National Laboratories, Livermore, CA 94550.
- (2) Bruce, T. C.; Pandit, U. K. The Effect of Geminal Substitution Ring Size and Rotamer Distribution on the Intramolecular Nucleophilic Catalysis of the Hydrolysis of Monophenyl Esters of Dibasic Acids and the Solvolysis of the Intermediate Anhydrides. *J. Am. Chem. Soc.* **1960**, *82*, 5858–5865.
- (3) Hillery, P. S.; Cohen, L. A. Stereopopulation Control. 9. Rate and Equilibrium Enhancement in the Lactonization of (*o*-Hydroxyphenyl)acetic Acids. *J. Org. Chem.* **1983**, *48*, 3465–3471 and references therein.

- (4) Kirby, A. J. Effective Molarities for Intramolecular Reactions. *Adv. Phys. Org. Chem.* **1980**, *17*, 183–278.
- (5) Menger, F. M. On the Source of Intramolecular and Enzymatic Reactivity. *Acc. Chem. Res.* **1985**, *18*, 128–134.
- (6) Page, M. I.; Jencks, W. P. Entropic Contributions to Rate Accelerations in Enzymic and Intramolecular Reactions and the Chelate Effect. *Proc. Natl. Acad. Sci. U.S.A.* **1971**, *68*, 1678–1683.
- (7) Houk, K. N.; Tucker, J. A.; Dorigo, A. E. Quantitative Modeling of Proximity Effects on Organic Reactivity. *Acc. Chem. Res.* **1990**, *23*, 107–113.
- (8) Lightstone, F. C.; Bruice, T. C. Ground State Conformations and Entropic and Enthalpic Factors in the Efficiency of Intramolecular and Enzymatic Reactions. 1. Cyclic Anhydride Formation by Substituted Glutarates, Succinate, and 3,6-Endoxo- Δ^4 -tetrahydrophthalate Monophenyl Esters. *J. Am. Chem. Soc.* **1996**, *118*, 2595–2605.
- (9) Lightstone, F. C.; Bruice, T. C. Separation of Ground State and Transition State Effects in Intramolecular and Enzymatic Reactions. 2. A Theoretical Study of the Formation of Transition States in Cyclic Anhydride Formation. *J. Am. Chem. Soc.* **1997**, *119*, 9103–9113.
- (10) Lightstone, F. C.; Zheng, Y.-J.; Bruice, T. C. Molecular Dynamics Simulations of Ground and Transition States for the S_N2 Displacement of Cl^- from 1,2-Dichloroethane at the Active site of Xanthobacter Autotrophicus Haloalkane Dehalogenase. *J. Am. Chem. Soc.* **1998**, *120*, 5611–5621.
- (11) Warshel, A. *Computer Modeling of Chemical Reactions in Enzymes and Solutions*; John Wiley & Sons: New York, 1991.
- (12) Schiøtt, B.; Iversen, B. B.; Madsen, G. K. H.; Bruice, T. C. On the Electronic Nature of Low-Barrier Hydrogen Bonds. *Proc. Natl. Acad. Sci. U.S.A.* **1998**, *95*, 12799–12802.
- (13) Saunders, M. Stochastic Exploration of Molecular Mechanics Energy Surfaces. Hunting for the Global Minimum. *J. Am. Chem. Soc.* **1987**, *109*, 3150–3152.
- (14) Saunders, M. Stochastic Search for the Conformations of Bicyclic Hydrocarbons. *J. Comput. Chem.* **1989**, *10*, 203–208.
- (15) Allinger, N. L.; Zhu, Z.-Q. S.; Chen, K. Molecular Mechanics (MM3) Studies of Carboxylic Acids and Esters. *J. Am. Chem. Soc.* **1992**, *114*, 6120–6133.
- (16) Illuminati, G.; Mandolini, L. Ring Closure Reactions of Bifunctional Chain Molecules. *Acc. Chem. Res.* **1981**, *14*, 95–102.
- (17) Lightstone, F. C.; Bruice, T. C. Enthalpy and Entropy in Ring Closure Reactions. *Bioorg. Chem.* **1998**, *26*, 193–199.
- (18) Bruice, T. C.; Benkovic, S. J. The Compensation in ΔH^\ddagger and ΔS^\ddagger Accompanying the Conversion of Lower Order Nucleophilic Displacement Reactions to Higher Order Catalytic Processes. The Temperature Dependence of the Hydrazinolysis and Imidazole-Catalyzed Hydrolysis of Substituted Phenyl Acetates. *J. Am. Chem. Soc.* **1964**, *86*, 418–426.
- (19) Frisch, M. J.; Pople, J. A.; Binkley, J. S. Self-Consistent Molecular Orbital Methods 25: Supplementary Functions for Gaussian Basis Sets. *J. Chem. Phys.* **1984**, *80*, 3265–3269.
- (20) Clark, T.; Chandrasekhar, J.; Spitznagel, G. W.; Shleyer, P. v. R. Efficient Diffuse Function-Augmented Basis Set for Anion Calculations. III. The 3-21+G Basis Set for First-Row Elements, Li–F. *J. Comput. Chem.* **1983**, *4*, 294–301.
- (21) Frisch, M. J.; Pople, J. A.; *et al.* *Gaussian 94*; Gaussian, Inc.: Pittsburgh, PA, 1995.
- (22) Jencks, W. P. *Catalysis in Chemistry and Enzymology*; McGraw-Hill Book Co.: New York, 1969.
- (23) Gonzalez, C.; Schlegel, H. B. An Improved Algorithm for Reaction Path Following. *J. Chem. Phys.* **1989**, *90*, 2154–2161.
- (24) Gonzalez, C.; Schlegel, H. B. Reaction Path Following in Mass-Weighted Internal Coordinates. *J. Phys. Chem.* **1990**, *94*, 5523–5527.
- (25) Wiberg, K. B.; Keith, T. A.; Frisch, M. J.; Murcko, M. Solvent Effects on 1,2-Dihaloethane Gauche/Trans Ratios. *J. Phys. Chem.* **1995**, *99*, 9072–9079.
- (26) Wiberg, K. B.; Rablen, P. R.; Rush, D. J.; Keith, T. A. Amides. 3. Experimental and Theoretical Studies of the Effect of the Medium on the Rotational Barriers for N, N-Dimethylformamide and N, N-Dimethylacetamide. *J. Am. Chem. Soc.* **1995**, *117*, 42.
- (27) Wiberg, K. B.; Castejon, H.; Keith, T. A. Solvent Effects. 6. A Comparison Between Gas Phase and Solution Acidities. *J. Comput. Chem.* **1996**, *17*, 185–190.
- (28) Becke, A. D. Density-Functional Thermochemistry. III. The Role of Exact Exchange. *J. Chem. Phys.* **1993**, *98*, 5648–5652.
- (29) Schiøtt, B.; Zheng, Y.-J.; Bruice, T. C. Theoretical Investigation of the Hydride Transfer from Formate to NAD^+ and the Implications for the Catalytic Mechanism of Formate Dehydrogenase. *J. Am. Chem. Soc.* **1998**, *120*, 7192–7200.
- (30) Zheng, Y. J.; Bruice, T. C. A Theoretical Examination of the Factors Controlling the Catalytic Efficiency of a Transmethylation Enzyme: Catechol O-Methyltransferase. *J. Am. Chem. Soc.* **1997**, *119*, 8137–8145.
- (31) Shaik, S. S.; Schlegel, H. B.; Wolfe, S. *Theoretical Aspects of Physical Organic Chemistry. The S_N2 Mechanism*; John Wiley & Sons: New York, 1992.
- (32) Verschuere, K. H. G.; Franken, S. M.; Rozeboom, H. J.; Kalk, K. H.; Dijkstra, B. W. Refined X-ray Structures of Haloalkane Dehalogenase at pH 6.2 and pH 8.2 and Implications for the Reaction Mechanism. *J. Mol. Biol.* **1993**, *232*, 856–872.
- (33) Verschuere, K. H. G.; Seljée, F.; Rozeboom, H. J.; Kalk, K. H.; Dijkstra, B. W. Crystallographic Analysis of the Catalytic Mechanism of Haloalkane Dehalogenase. *Nature* **1993**, *363*, 693–698.
- (34) Cornell, W. D.; Cieplak, P.; Bayly, C. I.; Gould, I. R.; Merz, K. M., Jr.; Ferguson, D. M.; Spellmeyer, D. C.; Fox, T.; Caldwell, J. W.; Kollman, P. A. A Second Generation Force Field For the Simulation of Proteins and Nucleic Acids. *J. Am. Chem. Soc.* **1995**, *117*, 5179–5197.
- (35) Maulitz, A. H.; Lightstone, F. C.; Zheng, Y.-J.; Bruice, T. C. Nonenzymatic and Enzymatic Hydrolysis of Alkyl Halides: A Theoretical Study of the S_N2 Reactions of Acetate and Hydroxide Ions with Alkyl Chlorides. *Proc. Natl. Acad. Sci. U.S.A.* **1997**, *94*, 6591–6595.
- (36) Stewart, J. J. P. Optimization of Parameters for Semiempirical Methods. I. Methods. *J. Comput. Chem.* **1989**, *10*, 209–220.
- (37) Lightstone, F. C.; Zheng, Y.-J.; Maulitz, A. H.; Bruice, T. C. Nonenzymatic and Enzymatic Hydrolysis of Alkyl Halides: A Haloalkane Dehalogenation Enzyme Evolved to Stabilize the Gas-Phase Transition State of an S_N2 Displacement Reaction. *Proc. Natl. Acad. Sci. U.S.A.* **1997**, *94*, 8417–8420.
- (38) Almarsson, Ö.; Karaman, R.; Bruice, T. C. Kinetic Importance of Conformations of Nicotinamide Adenine Dinucleotide in the Reactions of Dehydroge-

- nase Enzymes. *J. Am. Chem. Soc.* **1992**, *114*, 8702–8704.
- (39) Almarsson, Ö.; Bruice, T. C. Evaluation of the Factors Influencing Reactivity and Stereospecificity in NAD(P)H Dependent Dehydrogenase Enzymes. *J. Am. Chem. Soc.* **1993**, *115*, 2125–2138.
- (40) Almarsson, Ö.; Sinha, A.; Gopinath, E.; Bruice, T. C. Mechanism of One-Electron Oxidation of NAD(P)H and Function of NADPH Bound to Catalase. *J. Am. Chem. Soc.* **1993**, *115*, 7093–7102.
- (41) Luo, J.; Bruice, T. C. Molecular Dynamics Sampling on the Active Sites of the Dimeric HLADH/NADH/Benzaldehyde and the HLADH/NAD⁺/Benzalcohol Complex. To be published.

AR960131Y